Ultramicroscopy 147 (2014) 149–155

Contents lists available at ScienceDirect

Ultramicroscopy

journal homepage: www.elsevier.com/locate/ultramic

Practical aspects of the use of the X^2 holder for HRTEM-quality TEM sample preparation by FIB

Willem van Mierlo [a,*], Dorin Geiger [a], Alan Robins [b], Matthias Stumpf [b], Mary Louise Ray [b], Paul Fischione [b], Ute Kaiser [a]

[a] Materialwissenschaftliche Elektronenmikroskopie, University of Ulm, Germany
[b] E.A. Fischione Instruments, Inc., 9003 Corporate Circle, Export, PA 15632, USA

ARTICLE INFO

Article history:
Received 17 January 2014
Received in revised form
7 August 2014
Accepted 11 August 2014
Available online 20 August 2014

Keywords:
FIB
TEM specimen preparation
Sample thickness
Backscattered electrons
EDX
Monte
Carlo simulations
Sub-kV argon milling

ABSTRACT

The X^2 holder enables the effective production of thin, electron transparent samples for high-resolution transmission electron microscopy (HRTEM). Improvements to the X^2 holder for high-quality transmission electron microscopy (TEM) sample preparation are presented in this paper. We discuss the influence of backscattered electrons (BSE) from the sample holder in determining the lamella thickness in situ and demonstrate that a significant improvement in thickness determination can be achieved by comparatively simple means using the relative BSE intensity. We show (using Monte Carlo simulations) that by taking into account the finite collection angle of the electron backscatter detector, an approximately 20% underestimation of the lamella thickness in a silicon sample can be avoided. However, a correct thickness determination for light-element lamellas still remains a problem with the backscatter method; we introduce a more accurate method using the energy dispersive X-ray spectroscopy (EDX) signal for in situ thickness determination. Finally, we demonstrate how to produce a thin lamella with a nearly damage-free surface using the X^2 holder in combination with sub-kV polishing in the Fischione Instruments' NanoMill® TEM specimen preparation system.

1. Introduction

Enormous improvement in TEM instrument resolution due to hardware aberration correction [1,2] has resulted in a growing demand for the preparation of high quality TEM samples for high-resolution experiments. A consequence of aberration-correction is that lower voltages can achieve atomic resolution imaging; however, such applications require even thinner and higher quality TEM samples [3,4]. During the last decade, focused ion beam (FIB) devices have proven themselves to be practical tools for TEM sample preparation where sub-micron level sample location precision is required. Thin, HRTEM-quality samples are now prepared using standard sample preparation techniques involving mechanical dimpling followed by ion polishing [5], crushing of the sample material and dispersing it upon a support grid [6], or electropolishing [6].

There are also situations that may require FIB preparation of a very thin sample for HRTEM experiments, such as when mechanical treatment of the specimen is undesirable or charging effects necessitate a small TEM sample. Preparation of such thin lamellae requires a significant amount of operator experience. Even for an experienced operator, it can be difficult to obtain good, thin lamellae because of shrinking and bending of the lamella during the final stages of preparation. While shrinkage can be countered by depositing a very thick protective layer on the lamella [7], bending of the lamella presents a more serious obstacle because it is related to internal stresses [8] and surface stresses generated by ion impact [9,10], which are unavoidable during sample preparation by any ion beam technique.

Recently, a tiltable sample holder (the X^2 holder) that facilitates an effective fabrication of almost plan-parallel and ultra-thin TEM lamella [4] was developed by our group. Making large area, thin, HRTEM-quality samples, however, requires in situ monitoring of the specimen thickness during milling. The accurate determination of the sample thickness was still an open question with this holder. This article will go deeper into sample geometry effects on the determination of lamella thickness in combination with the new holder using the BSE signal [11]. A new technique, based on the intensity of a characteristic X-ray peak that overcomes many of the problems imposed by sample geometry on the BSE technique, is also presented.

During conventional FIB lamella preparation, determining the thickness of a lamella inside of the FIB is also desirable. Controlling

* Corresponding author. Present address: Johnson Matthey Technology Centre, Blount's Court, Sonning Common, Reading, RG4 9NH, United Kingdom.
E-mail address: VanmiW01@matthey.com (W. van Mierlo).

http://dx.doi.org/10.1016/j.ultramic.2014.08.007
0304-3991/

the thickness of the specimen is generally important because different TEM techniques have different requirements regarding the optimal thickness. For example, in core-loss energy-filtered transmission electron microscopy (EFTEM), the sample is ideally thicker than for HRTEM because the core-loss signal is relatively weak – especially for high-energy edges. Kothleitner and Hofer [12] suggest an optimal thickness of approximately $0.4\times$ the inelastic mean free path for the carbon K-edge in titanium carbide, which would correspond to an optimal thickness of 50–55 nm at 200 kV. Classical TEM also requires thicker samples because surfaces may interact with dislocations and other defects [6]. On the opposite end of the spectrum, low-voltage HRTEM imaging requires extremely thin lamellae. A better control on lamella thickness would be beneficial to all these applications.

Milling at higher beam energies usually increases milling rates and results in a more precise beam. However, higher beam energies generate damage deeper in the sub-surface of the lamella that results in thicker damage layers [13]. Therefore, switching to a lower beam energy is ideally done at a lamella thickness of the final required thickness, plus the depth to which the damage extends for a particular beam energy. Lateral variations in thickness can often be corrected during FIB preparation by adjusting the beam scanning rotation angle or tilt angle of the specimen holder. A better in situ, lateral resolved thickness determination will benefit TEM-lamella preparation by FIB.

We will show an application example where an almost surface-damage-free TEM lamella has been produced using sub-kV, post-FIB, argon polishing.

2. Method description

Using the X^2 sample holder, which is described in more detail in [4], the sample can be flipped 90° inside the FIB/SEM. This makes it possible to cut two perpendicular grooves on either side of the lamella, which creates an electron transparent window at the intersection of the grooves. When this technique is compared to the conventional FIB-preparation technique, the major difference is that thick portions of the lamella remain on all four sides of the electron transparent area. These thick portions form a rigid frame that supports the electron transparent area. The frame greatly reduces the shrinking and bending of the lamella that is commonly observed during the final stages of thin lamella preparation.

Improvements to the sample holder include a 1.5 mm lowering of the mechanical tilt axis, which allows the stage to tilt to higher angles and makes the preparation of TEM lamellae easier. In addition, organic tape was added to the sample holder head to reduce the amount of back scattered electrons from the sample holder and to make it easier to determine the lamella thickness (described below).

The lamella thickness is estimated in conventional FIB-preparation method from the top view cross section of the lamella. However, this is not possible when using the X^2 method, because the view on the electron transparent area is obstructed by the thick frame around it. In addition, the accuracy for the cross-section view method is limited by the ion beam width, the accuracy with which one can orientate the lamella parallel to the ion beam, and the beam convergence angle. Assuming optimal conditions (an unbent lamella, 15 nm beam width, 0.1° orientation accuracy and 1 mrad full convergence angle [14]), one obtains an accuracy of ~20 nm for a 5 μm high lamella. For the fabrication of high-resolution TEM quality lamellae, this means that the method's uncertainty is roughly equal to the desired thickness. This method is only able to measure the thickest part of the lamella; local thickness variations cannot be determined. Therefore, while using the X^2 method, we also use another method, which is based on the intensity of the lamella's BSE signal.

2.1. Thickness determination using BSE-intensity

The ratio of BSE intensity between bulk and film samples can be used to infer the thickness of a film lying on a substrate [15,16]. Salzer et al. [11] have applied a similar technique where parameterized results of Monte Carlo simulations have been used to measure the thickness of a free-standing TEM lamella. The precision of Monte Carlo simulations for BSE-related parameters (e.g., backscatter yield and BSE distribution) typically lies is the range of ~20% for aluminium and increases with atomic weight to below 5% for gold [17,18]. A correct determination of the lamella thickness using the BSE method requires the measurement of the BSE intensity at a position where the thickness of the lamella is greater than the maximum penetration depth of the incident electrons (bulk intensity) and at a position where the intensity corresponds to a lamella of 0 nm thickness (background intensity). The latter can be measured at a position 'in the vacuum' next to the lamella. However, the vacuum around the lamella is not a real vacuum, but usually at approximately one millimetre behind the lamella, there is a part of the sample holder in the background. The sample holder therefore generates BSE that are detected by the BSE detector. The electrons that are transmitted through the electron transparent window and reach the sample holder have an angular distribution that is very different from those that directly hit the sample holder, i.e., the background measurement, due to strong scattering within the lamella, as shown by Monte Carlo simulations. Therefore, the vacuum BSE intensity is generally different from the background BSE intensity.

Monte Carlo simulations on a silicon lamella were performed at 5 kV beam energy; the geometry of the sample holder and the detector were taken into account. Most sample holders are made out of aluminium or are gold plated – the latter to reduce charging effects. Results indicate that when a gold-plated sample holder is directly exposed to the incident beam, the BSE background signal is about 1.5 times higher than the BSE signal coming from the thick (bulk) part of the lamella. For an aluminium sample holder, this reduces about half of the bulk intensity, which is, although smaller, still significant. This makes the method inaccurate for most sample holders, as it relies heavily on a correct determination of the bulk thickness intensity and background intensity and is, in fact, useless for light-element lamellae. One can only use the BSE method as a reliable method for thickness determination when the BSE intensity from the sample holder is minimized. Because organic materials have a low mean atomic number, carbon-coated tape has been put on the part of the sample holder that is visible in the SEM view during the final stages of milling to minimize the amount of BSE coming from the sample holder. Again, Monte Carlo simulations indicate that when a polyethylene-based tape is used to cover the sample holder head, a more than seven-fold reduction in the BSE background signal is expected when compared to an uncovered, gold-plated sample holder. The reduction of the background BSE signal is demonstrated in Fig. 1.

Fig. 2 shows the result of Monte Carlo simulations on the relative intensity of the BSE signal of the thin part of the lamella (relative to the difference between the bulk intensity and the background intensity) as a function of the electron-transparent-area thickness. Curves for three geometries are displayed. The solid line represents the BSE intensity in the absence of a holder, i.e., it represents a geometry that can be simulated easily in standard Monte Carlo software. The short dashed line represents the sample holder covered by tape and the long dashed line represents the sample holder not covered, i.e., the electron beam strikes the gold-plated holder directly.

When the gold-plated sample holder is not covered by tape, a monotonic increase of the BSE intensity with sample thickness is not observed, making thickness determination based on this

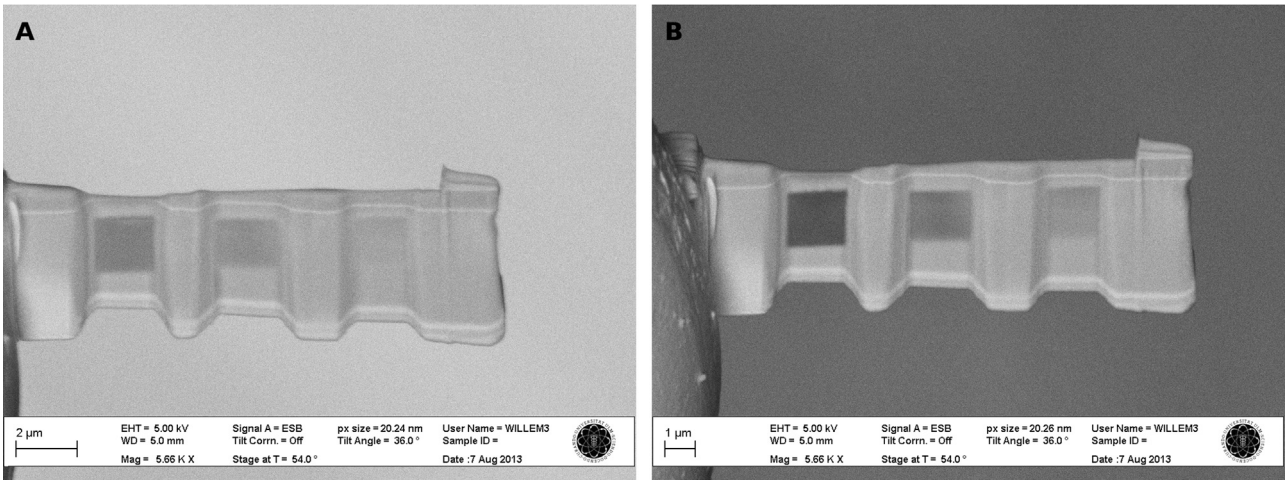

Fig. 1. A BSE image of a FIB-prepared TEM lamella taken without covering the gold-plated sample holder with tape (A) and after covering the holder with an organic tape (B). Note the difference in background intensity next to the TEM lamella in both cases. Images were taken at the same acceleration voltage, beam current, brightness settings, and contrast settings. The lamella material is silicon; window thickness (dark squares inside of the lamella) increases from left to right.

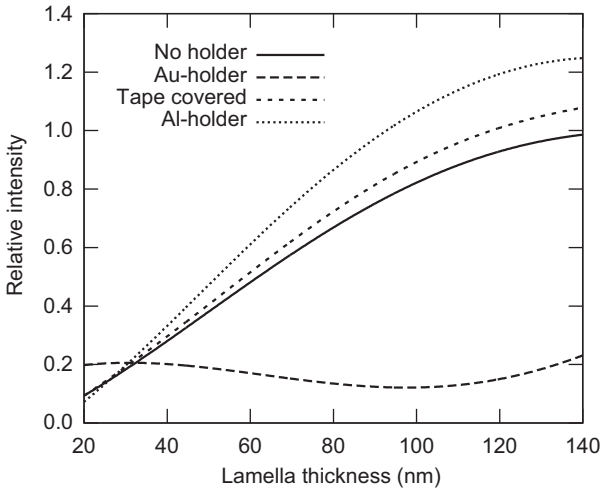

Fig. 2. Relative intensity of the BSE signal as a function of thickness of the electron transparent area of a silicon lamella when using different types of holders. Simulation conditions were 5 kV beam energy and 36° angle of incidence.

method impossible. An aluminium holder looks better; however, at a relative intensity of 50% the error is still 20% and increases for higher relative intensities. When the sample head is covered by a polyethylene-based tape, below a relative intensity of 100% a monotonic increase with thickness is observed. However, the discrepancy between the simple sample geometry without holder and the actual geometry again increases with thickness. Below a relative intensity of 60%, the discrepancy is below 10% and thus comparable with the accuracy of thickness determination by electron energy loss spectroscopy (EELS) when the holder-less geometry is used as input for the Monte Carlo simulations.

All simulations were performed with a $5 \times 5\ mm^2$ holder positioned 775 µm below the lamella and with the lamella front- and back-side surfaces perpendicular to the holder surface. The BSE detector is modelled as a circular inlens detector, where the apparent detector size is defined by the bore size of the objective pole piece (8 mm diameter). The software used for the simulation was an adapted version of NistMonte/DTSA-II [19].

A second effect one should be aware of is the finite collection angle of the BSE detector. Fig. 3 shows the result of a 5 million-electron Monte Carlo simulation. For each BSE, the maximum depth in the sample and the backscatter angle (the angle at which the BSE is leaving the sample relative to the incident electron beam) was tracked. The Monte Carlo simulations specified a 36° angle of incidence.

The results show that the backscatter angle depends on the maximum depth of a BSE that penetrates the sample. As BSE detectors generally collect BSE relatively close to the incident beam, comparing the measured intensity with a full Monte Carlo simulation would yield results that underestimate the true thickness by ~20% at relative BSE intensities between 20% and 80% (Fig. 3b). Simulations have been performed for a silicon lamella at 10 kV and 2 kV (Fig. 3 shows the results at 2 kV) and the simulations show essentially the same behaviour – a 20% underestimation of the true lamella thickness. A correct determination of lamella thickness, therefore, requires a Monte Carlo simulation that takes into account the dependence of the backscatter angle on the maximum depth of electron penetration into the target. However, our results show that adding 20% to the determined depth from a standard Monte Carlo simulation also gives a reasonably good thickness estimate.

2.2. Thickness determination using EDX

As explained in the previous section, the relative BSE intensity of the electron transparent window is an easy way to measure the thickness of the electron transparent windows in the lamella. However, the unknown background intensity makes it difficult when the BSE intensity of the vacuum measured next to the lamella is similar, or even higher, than the intensity of the thin part of the lamella. Therefore, an alternative method is presented; the thickness is determined by the relative intensity of a single characteristic X-ray peak, which is measured using an energy dispersive spectroscopy (EDX) detector. The accuracy of Monte Carlo methods to model the X-ray signal of thin films on a substrate is about 10% for beam energies below 10 kV [20] and is, therefore, comparable to that of EELS. The measured relative intensity is then compared to Monte Carlo simulation of thin films of different thicknesses. The main advantage of this method is that it is much easier to distinguish between the signal from the lamella itself and from the sample holder, as long as the specimen has an element that is not present in the sample holder and characteristic X-ray peaks in a region where the Bremmstrahlung background can easily be corrected for. Though making thickness maps is more time consuming with this method, as with the BSE method (about 50–100 times slower), the accuracy of this method

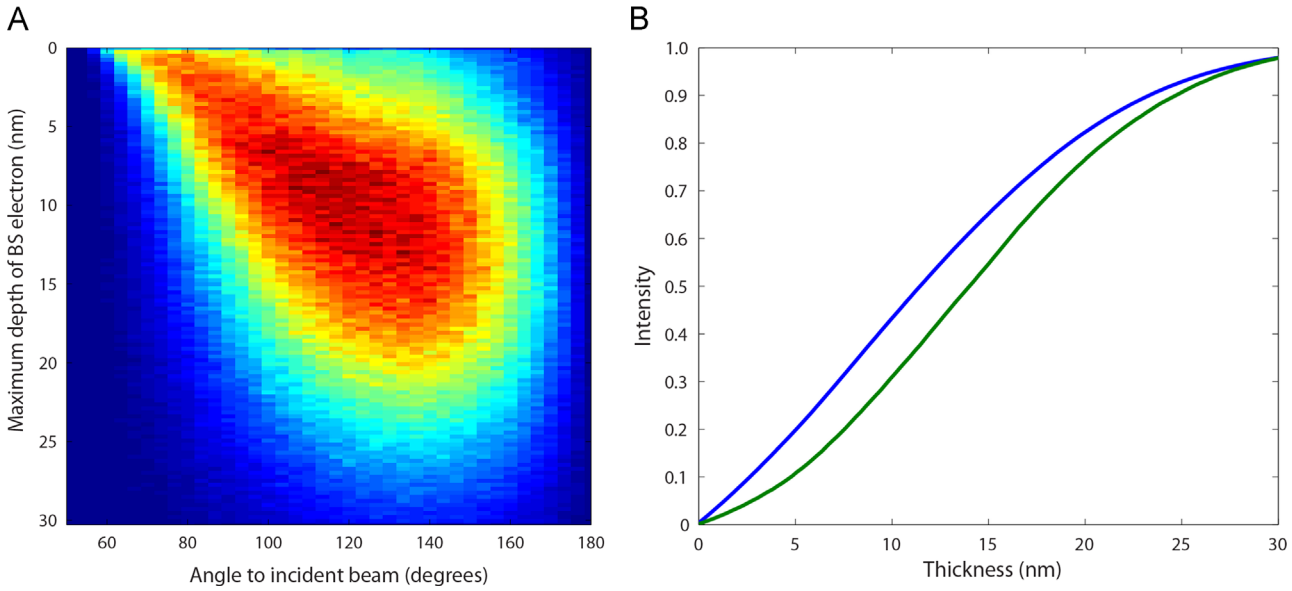

Fig. 3. (A) The relationship between the angle at which a BSE leaves the sample relative to the incident beam and the maximum depth of the electron penetration of the target. The more the angle is anti-parallel to the incident beam, the deeper the average penetration depth. (B) The BSE intensity as a function of lamella thickness showing the effect of back detector position and collection angle. It shows that not taking into account the detector position leads to a ~20% underestimation of lamella thickness. The blue line shows all BSEs; the green line shows only BSEs with an angle above 150° relative to the incident beam. (For interpretation of the references to colour in this figure legend, the reader is referred to the web version of this article.)

is higher, because of the easy discrimination between the lamella and holder signal. The depth range to which this method is sensitive is generally larger than for the BSE method, because the total extent of the interaction volume is larger than the maximum depth that a BSE penetrates the target. The maximum thickness to which this method is usable is controlled by the acceleration voltage used to measure the thickness, thicker samples generally need a high acceleration voltage. Ideally, the characteristic X-ray intensity of the electron transparent part is 20–80% of the bulk part (thick) of the lamella.

Fig. 4 shows the result for the summed relative GaLα and GaLβ intensity, calculated by Monte Carlo simulations for GaN using a 5 kV incident beam.

As expected, the relative intensity shows a monotonic increase with thickness, and thus, the thickness can be estimated from the relative intensity of the X-ray peak. Fig. 5 shows a FIB-prepared lamella of a GaN LED-structure cross section with the corresponding spectra taken at a position where the thickness is greater than the extent of the interaction volume (spectrum 2) and at the tip of the GaN triangle (spectrum 1). Because the window is thinner than the interaction volume at 5 kV, it shows a reduced intensity of the gallium L-peaks. The relative intensity at the ET window position is 41.6%, which can be read from Fig. 4 to correspond to a thickness of 39 nm. The thickness at the same position has been estimated to be 38 nm from the EELS low-loss spectra [21]. Thickness determination using the BSE method without correction for detector collection angle gave a thickness of 44 nm (~16% overestimation relative to the EELS estimate), again showing that for an accurate determination, one needs to take into account the influence of the BSE detector collection angle. Spectrum 3 in Fig. 5 was taken at the base of the pyramid, about 3 μm away from point 1, and has a relative intensity of 51%, which gives a thickness of 48 nm. This results show that the wedge angle of the electron transparent window is below 0.2°. Fig. 5c–e shows HRTEM images of a similarly prepared TEM lamella demonstrating that the transparent area is of a suitable uniform thickness to obtain lattice fringes over the complete electron transparent window.

Before the EDX measurements were taken, the measured surfaces were polished with a 5 kV Ga beam. From TRIM simulations [22], we estimate that this reduces the thickness of the Ga^+ implantation layer to about 5 nm. From Monte Carlo simulations on characteristic X-ray production, we estimate that influence of the implantation layer on the determined thickness is below 2%.

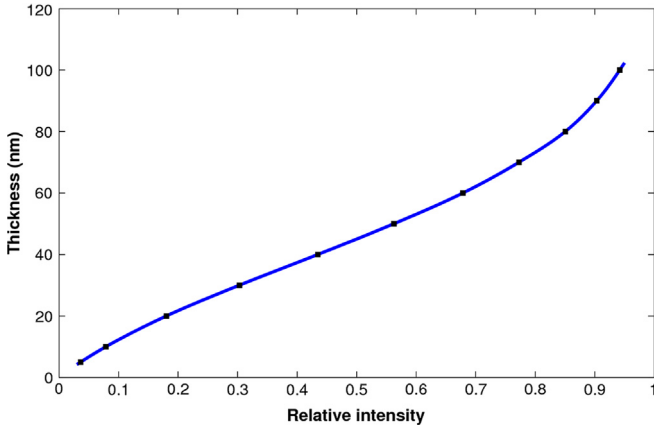

Fig. 4. Relative characteristic X-ray (sum of GaLα and GaLβ) intensity of GaN as estimated from Monte Carlo simulations (the bulk sample has an intensity of 100%). Acceleration voltage is 5 kV, incident angle is 0°.

These results shows that the EDX method for the determination of lamella thickness gives reliable results and thus can be used as a more precise, albeit slower, method for the in situ thickness determination during FIB preparation. Although EDX analyses after TEM lamella preparation may cause contamination of the samples; plasma cleaning is an effective way of removing contamination for materials that are suitable for plasma cleaning. Our experience is that plasma cleaning after the FIB preparation removes majority of the contamination.

Accurate lateral resolved thickness measurements, either by the BSE method or EDX, make it possible to correct lateral thickness differences by adjusting the beam scan rotation and stage tilt angles. When combined with the increased lamella stability from the X^2 method, it can be used to produce large area, electron transparent lamellae by FIB.

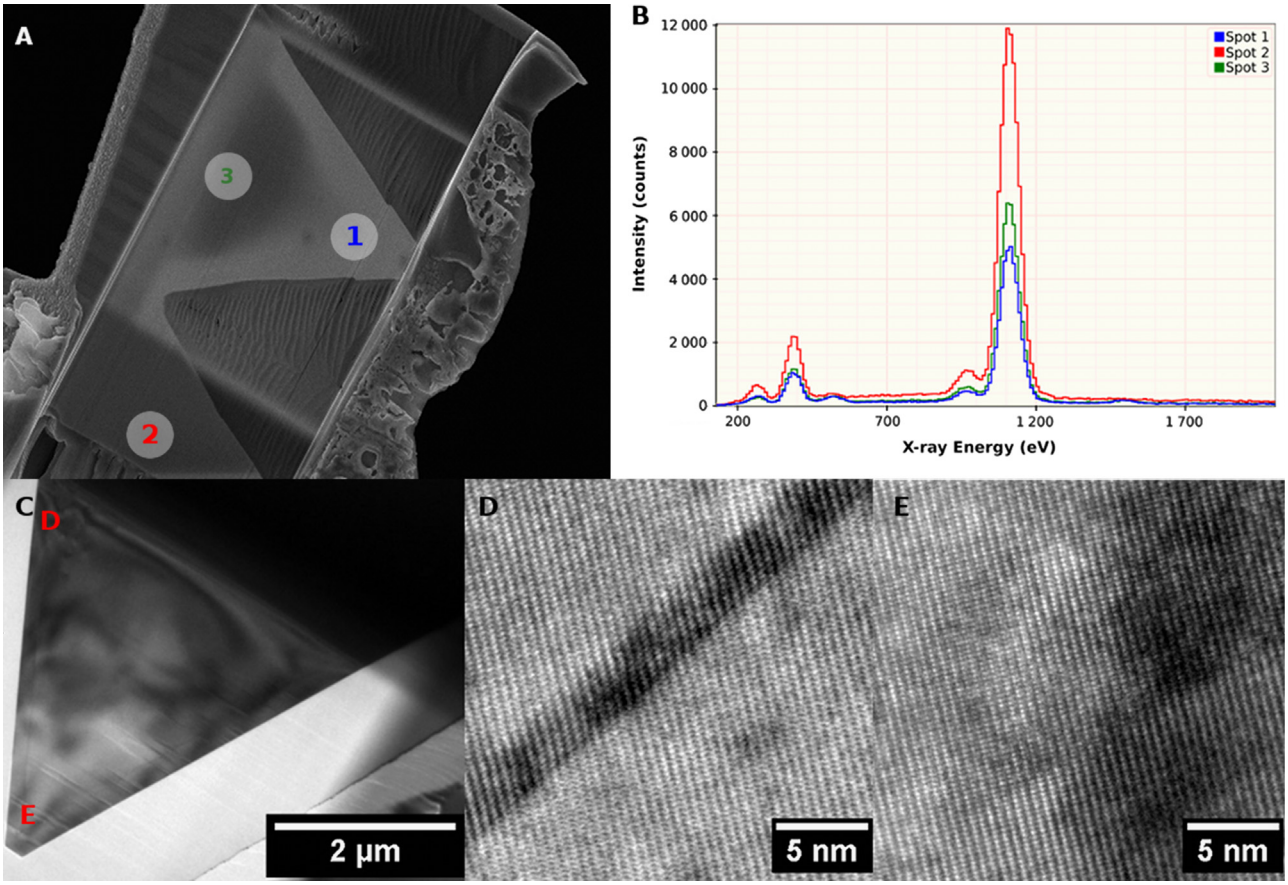

Fig. 5. (A) SEM image of GaN-pyramid lamella with the locations the EDX analyses indicated. (B) EDX spectra of both locations showing the decreased X-ray signal at the electron transparent window (1 and 3) as compared to the location where the lamella thickness is greater than the extent of the interaction volume (2). Spectra were measured using the same live time and a dead time below 10%. (D) Overview TEM image of a similarly prepared TEM-lamella approximately 35 nm thick. The red D and E indicate the location of HRTEM images D and E. (E) HRTEM image taken at 200 kV near the base of the pyramid and near the tip of the pyramid. (For interpretation of the references to colour in this figure legend, the reader is referred to the web version of this article.)

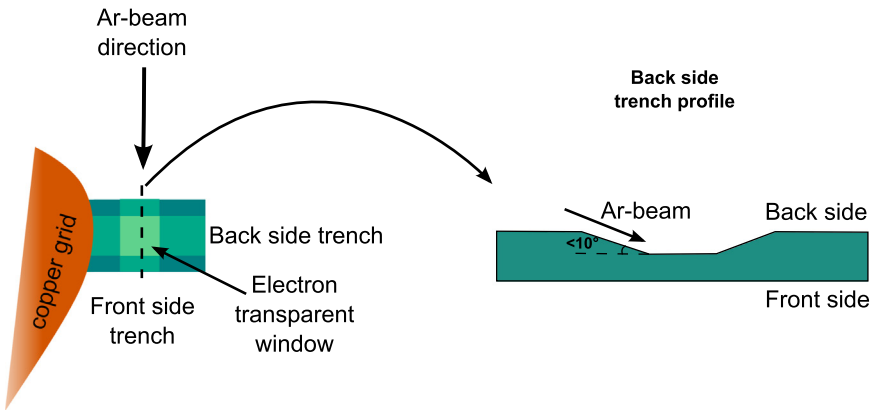

Fig. 6. Illustration of the trench geometry required for use of the X^2 holder in combination with the NanoMill® TEM specimen preparation system. To access the electron transparent window with the argon beam, the side wall of the trench on the back side of the lamella, (the trench in the long direction of the lamella) must have an angle below 10°.

3. Post-FIB argon polishing

We showed that with the proposed improvements to the thickness determination techniques it is possible to produce large area, thin TEM lamella by FIB. However, it is well know that TEM sample preparation by FIB causes implantation of gallium in the surface layers, as well as amorphization of the surface layers. This has a detrimental effect on the quality of the TEM experiment. This is especially true as the lamella gets thinner (which is necessary for lower accelerating voltages of the TEM); the influence of the amorphous surface layer has a large effect on the HRTEM image quality [23]. Low-voltage, post-FIB argon polishing has shown that it can significantly increase the quality of TEM specimens [24].

A major problem associated with post-FIB argon polishing is that most argon milling devices have a relative broad beam – usually significantly broader than the lamella size. Because of this, not only the lamella is milled, but also the (copper) grid holding the lamella. This leads to redeposition of copper onto the lamella.

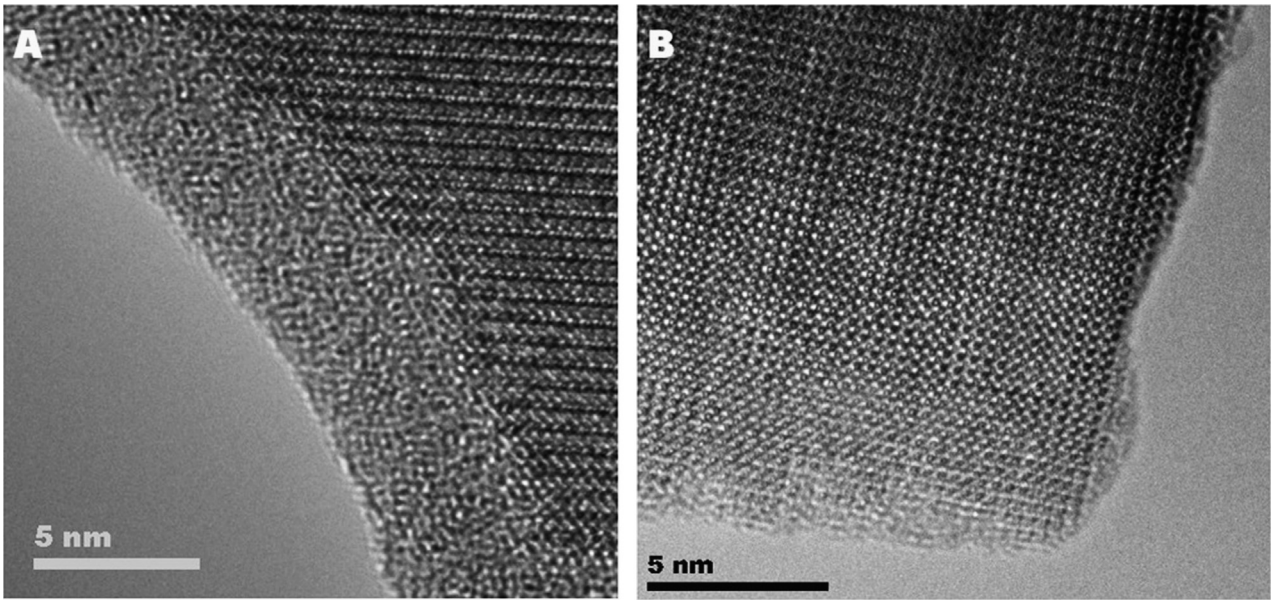

Fig. 7. (A) The damage layer after FIB polishing at 5 kV can be observed as an amorphous hole near the edge of the sample. (B) Results after polishing with a 500 V argon beam in the Fischione Instruments' NanoMill® TEM specimen preparation system. Lattice fringes can be observed up to the edge of the sample, which indicates that the damage layer has been almost completely removed.

From our experience, instead of increasing the lamella quality, broad beam Ar ion milling actually decreases the quality of the lamella. The Fischione NanoMill argon milling device has a beam diameter of approximately 1 μm [25], which is significantly smaller than the size of the TEM lamella. Therefore, no milling of the copper grid occurs and no redeposition is expected. A minor modification to the sample preparation, however, is required, as the sidewalls of the grooves that form the electron transparent window may block the argon beam from accessing the electron transparent portion of the sample. Therefore, one needs to make sure that the side walls on the side where the argon beam is perpendicular to the groove direction have an angle that is smaller than the glancing angle of the argon beam (usually 10°, see Fig. 6).

If the area of interest is the near-surface structure, a thicker than normal protection cap (2–3 μm) can be added to the lamella to ensure lamella stability.

Fig. 7 shows the results of sub-kV argon polishing of an X^2 prepared lamella. The lamella material is a $La_{0.29}Sr_{0.7}Al_{0.65}Ta_{0.35}O_3$ substrate with nickelate and aluminate heterostructures directly below the surface. The HRTEM images were taken on a C_s-corrected Titan 80–300 operated at 80 kV. Fig. 7a shows the edge of the sample after 5 kV FIB polishing. The edge shows a 5 nm thick amorphous rim, which indicates that a significant amorphous damage layer remains on the sample surfaces. Fig. 7b shows the results after 900 V argon polishing for 10 min, followed by 500 V argon polishing for 5 min on either side of the TEM lamella. As can be seen, the amorphous edge has been reduced to 1–2 layers of atoms at most locations, indicating that the amorphous implantation layer was almost completely removed by argon polishing. These results show that post-FIB argon polishing is possible with the X^2 technique after a minor modification of the groove geometry and, in fact, results in an increase in lamella quality. A fine argon beam is essential to obtain good results.

4. Summary

This paper evaluates two different methods that can be used to measure the thickness of a FIB-prepared lamella for TEM during preparation in the FIB. The backscatter method [11], in combination with the standard X^2 holder, has one major problem – the sample holder has been gold galvanized and, therefore, the background intensity is poorly defined. We show that covering the part of the sample holder that is visible during milling with a carbon-coated organic tape greatly reduces the background signal and, therefore, results in more reliable measurements of the sample thickness. The other method, which is a more precise, albeit slower, method for thickness determination is the use of the relative intensity of characteristic X-ray peaks. This method is shown to be more precise than the BSE method (2.6% difference between the EDX and EELS estimate vs. 15.8% difference BSE and EELS) because one can more easily discriminate between the X-ray signal coming back from the sample and X-ray signal coming back from the sample holder. Moreover, there is no problem with the detector collection angle. The increased accuracy in thickness determination makes it possible to produce large area, electron transparent, TEM lamellae by FIB. Finally, the use of the X^2 holder, in combination with the NanoMill system, to remove detrimental artifacts from the Ga milling process by sub-kV argon polishing shows that this combination can produce a TEM lamellae nearly absent of surface damage.

Acknowledgements

WM, DG, and UK are grateful to DFG (German Research Foundation) and the state of Baden Wuerttemberg for their support under the SALVE (Sub-Angstrom Low-Voltage Electron Microscopy) Project.

NanoMill is a registered trademark of E.A. Fischione Instruments, Inc.

References

[1] M. Haider, H. Rose, S. Uhlemann, E. Schwan, B. Kabius, K. Urban, A spherical-aberration-corrected 200 kV transmission electron microscope, Ultramicroscopy 75 (1998) 53–60. http://dx.doi.org/10.1016/S0304-3991(98)00048-5.

[2] O.L. Krivanek, N. Dellby, A.R. Lupini, Towards sub-Å electron beams, Ultramicroscopy 78 (1999) 1–11. http://dx.doi.org/10.1016/S0304-3991(99)00013-3.

[3] U. Kaiser, J. Biskupek, J.C. Meyer, J. Leschner, L. Lechner, H. Rose, et al., Transmission electron microscopy at 20 kV for imaging and spectroscopy, Ultramicroscopy 111 (2011) 1239–1246. http://dx.doi.org/10.1016/j.ultramic.2011.03.012.

[4] L. Lechner, J. Biskupek, U. Kaiser, Improved focused ion beam target preparation of (S)TEM specimen – a method for obtaining ultrathin lamellae, Microsc. Microanal. 18 (2012) 379–384. http://dx.doi.org/10.1017/S1431927611012499.
[5] Á. Barna, B. Pécz, M. Menyhard, TEM sample preparation by ion milling/amorphization, Micron 30 (1999) 267–276. http://dx.doi.org/10.1016/S0968-4328(99)00011-6.
[6] D.B. Williams, C.B. Carter, Transmission electron microscopy: a textbook for materials science, Springer Verlag, New York, 2009.
[7] H.-J. Kang, J. Kim, J. Oh, T. Back, H. Kim, Ultra-thin TEM sample preparation with advanced backside FIB milling method, Microsc. Microanal. 16 (2010) 170–171. http://dx.doi.org/10.1017/S1431927610054474.
[8] L.A. Giannuzzi, B. Kempshall, S.M. Schwarz, J.K. Lomness, B.I. Prenitzer, F.A. Stevie, FIB lift-out specimen preparation techniques, in: L.A. Giannuzzi, F.A. Stevie (Eds.), Introduction to Focused Ion Beams: Instrumentation, Theory, Techniques, and Practice, 1st ed.,Springer, New York, 2005, pp. 201–228.
[9] L. Pastewka, R. Salzer, A. Graff, F. Altmann, M. Moseler, Surface amorphization, sputter rate, and intrinsic stresses of silicon during low energy Ga^+ focused-ion beam milling, Nucl. Instrum. Methods Phys. Res. Sect. B: Beam Interact. Mater. Atoms 267 (2009) 3072–3075. http://dx.doi.org/10.1016/j.nimb.2009.06.094.
[10] R. Salzer, A. Graff, M. Simon, F. Altmann, Quantitative assessment of tem-sample warping caused by FIB preparation, Microsc. Microanal. 16 (2010) 172–173. http://dx.doi.org/10.1017/S1431927610061787.
[11] R. Salzer, A. Graff, M. Simon, F. Altmann, Standard free thickness determination of thin TEM samples via backscatter electron image correlation, Microsc. Microanal. 15 (2009) 340–341. http://dx.doi.org/10.1017/S1431927609096457.
[12] G. Kothleitner, F. Hofer, Optimization of the signal to noise ratio in EFTEM elemental maps with regard to different ionization edge types, Micron 29 (1998) 349–357. http://dx.doi.org/10.1016/S0968-4328(98)00014-6.
[13] J. Mayer, L.A. Giannuzzi, T. Kamino, J. Michael, TEM sample preparation and FIB-induced damage, MRS Bull. 32 (2007) 400–407.
[14] J. Orloff, L. Swanson, M. Utlaut, High Resolution Focused Ion Beams: FIB and Applications, 1st ed., Springer Verlag; New York, 2002.
[15] H. Niedrig, Film-thickness determination in electron microscopy: the electron backscattering method, Opt. Acta: Int. J. Opt. 24 (1977) 679–691. http://dx.doi.org/10.1080/713819609.
[16] O.S. Rajora, A.E. Curzon, A simple method for the determination of film thickness from electron image contrast in a scanning electron microscope, Thin Solid Films 123 (1985) 235–238. http://dx.doi.org/10.1016/0040-6090(85)90163-4.
[17] K. Murata, T. Matsukawa, R. Shimizu, Monte Carlo calculations on electron scattering in a solid target, Jpn. J. Appl. Phys. 10 (1971) 678–686. http://dx.doi.org/10.7567/JJAP.10.678.
[18] G. Love, M.G.C. Cox, V.D. Scott, A simple Monte Carlo method for simulating electron-solid interactions and its application to electron probe microanalysis, J. Phys. D: Appl. Phys. 10 (1977) 7. http://dx.doi.org/10.1088/0022-3727/10/1/002.
[19] N.W.M. Ritchie, Spectrum Simulation in DTSA-II, Microsc. Microanal. 15 (2009) 454–468. http://dx.doi.org/10.1017/S1431927609990407.
[20] P. Statham, P. Duncumb, Systematic discrepancies in Monte Carlo predictions for thin surface layers and visualisation to expose root causes, Microsc. Microanal. 16 (2010) 282–283. http://dx.doi.org/10.1017/S1431927610060927.
[21] R.F. Egerton, Electron Energy-Loss Spectroscopy in the Electron Microscope, 2nd ed., Plenum Press, New York, 1996.
[22] J.P. Biersack, L.G. Haggmark, A. Monte, Carlo computer program for the transport of energetic ions in amorphous targets, Nucl. Instrum. Methods 174 (1980) 257–269. http://dx.doi.org/10.1016/0029-554X(80)90440-1.
[23] M.L. Miller, R.C. Ewing, Image simulation of partially amorphous materials, Ultramicroscopy 48 (1993) 203–237. http://dx.doi.org/10.1016/0304-3991(93)90183-X.
[24] A. Genç, Post-FIB TEM sample preparation using a low energy argon beam, Microsc. Microanal. 13 (2007) 1520–1521. http://dx.doi.org/10.1017/S1431927607076064.
[25] R.R. Cerchiara, P.E. Fischione, J. Liu, J.M. Matesa, A.C. Robins, H.L. Fraser, et al., Raising the standard of specimen preparation for aberration-corrected TEM and STEM, Microsc. Today 19 (2011) 16–19. http://dx.doi.org/10.1017/S1551929510001197.